Synthesis and characterization of the layered iron-selenide $Na_{0.8}Fe_{1.6}Se_2$

Y. J. Long,[1,2] D. M. Wang,[1] Z. Wang,[2] H. X. Yang,[2] J. B. He,[1] L. X. Zhao,[2] P. P. Wang,[2] M. Q. Xue,[2] J. Q. Li,[2,3] Z. A. Ren,[2,3] and G. F. Chen[1,2,3,*]

[1]*Department of Physics, Renmin University of China, Beijing 100872, China*

[2]*Institute of Physics and Beijing National Laboratory for Condensed Matter Physics, Chinese Academy of Sciences, Beijing 100190, China*

[3]*Collaborative Innovation Center of Quantum Matter, Beijing 100190, China*

(Received 16 September 2014; revised manuscript received 15 October 2014; published 30 October 2014)

An iron-selenide $Na_{0.8}Fe_{1.6}Se_2$ single crystal has been successfully synthesized using a self-flux method. The electrical resistivity measurement shows that this material exhibits semiconducting behavior in the whole temperature range, with an anomalous increment of resistivity at $T_s \sim 595$ K. By varying the concentrations of Na and Fe, a small volume of superconducting phase could be achieved with a critical temperature of $T_c \sim 34$ K. Structural characterization shows that, similarly to $K_{0.8}Fe_{1.6}Se_2$, the $Na_{0.8}Fe_{1.6}Se_2$ phase exhibits clear superstructure with a modulation wave vector of $q = (3/5,1/5,0)$ caused by the Fe-vacancy order within the *a*-*b* plane.

DOI: 10.1103/PhysRevB.90.144519 PACS number(s): 74.70.Xa, 74.25.F−, 81.10.Jt, 61.72.−y

I. INTRODUCTION

The occurrence of superconductivity in the simple layered FeSe compound with the edge-sharing $FeSe_4$ tetrahedron has generated tremendous research interest. Bulk FeSe exhibits superconductivity with $T_c \sim 8$ K at ambient pressure [1], which can be dramatically raised up to ∼37 K with the application of high pressure [2]. Most surprisingly, a record high T_c of ∼65 K has been detected in the single-layer FeSe films grown on $SrTiO_3$ substrate [3]. By intercalating *Am* (*Am* = K, Rb, Cs, and Tl) between the FeSe layers, the superconductivity was observed at ∼30 K in $Am_{1-x}Fe_{2-y}Se_2$ [4–7]. Amazingly, these new superconductors exhibit several unique characteristics, such as the intrinsic vacancy ordering [8–10], the AFM ordering with an extremely large magnetic moment on the Fe site at a very high temperature just below the Fe-vacancy ordering temperature [10], and the absence of a holelike Fermi surface around the center of the Brillouin zone [11,12], which are present in the other iron-based superconductors and challenge the proposed pairing mechanism of interband scattering [13,14]. Later, intrinsic phase separation [15–17] was observed in these materials, which includes an AFM insulating/semiconducting phase with formula $Am_{0.8}Fe_{1.6}Se_2$ (the so called 245 phase), a metallic-superconducting phase with formula $Am_{1-x}Fe_2Se_2$ ($0 \leqslant x \leqslant 0.7$), and even another insulating/semiconducting phase with formula $AmFe_{1.5}Se_2$ (the so called 234 phase) [18]. Up to now, there are still unsettled issues [15,16,19] remaining controversial and requiring further research, especially the composition and nature of the superconducting phase, the relationship between the superconducting phase and the AFM phase, and the stoichiometry and magnetic ground state of the parent phase. In order to clarify these issues, it is crucial to improve the quality of the single-crystalline samples and to explore new isostructural iron chalcogenide superconductors and other related materials. Here, we report the detailed synthesis and characterization of iron-selenide $Na_{1-x}Fe_{2-y}Se_2$. Our result shows that $Na_{0.8}Fe_{1.6}Se_2$ behaves semiconducting and undergoes a Fe-vacancy order to disorder transition at about 595 K. And superconductivity with a critical temperature of $T_c \sim 34$ K can be achieved at certain composition, but as a small volume fraction coexisting with the $Na_{0.8}Fe_{1.6}Se_2$ phase in a phase-separated manner.

II. EXPERIMENTAL DETAILS

Single-crystalline samples of $Na_{1-x}Fe_{2-y}Se_2$ were prepared by the self-flux method. The starting material FeSe was first synthesized by reacting Fe powder (Alfa, 3N5) with Se powder (Alfa, 5N) at 400 °C for 200 h. Then, Na pieces (Alfa, 2N5) and FeSe powder were put into an alumina crucible with nominal composition $Na_{1-\delta}Fe_{2+\zeta}Se_2$ ($0 \leqslant \delta \leqslant 0.5$, $0 \leqslant \zeta \leqslant 0.5$), and the alumina crucible was evacuated and sealed into a thick-walled quartz tube. The quartz tubes were annealed at 700 °C over 20 h and cooled down to 400 °C at a rate of 3 °C/h. Platelike crystals of $Na_{1-x}Fe_{2-y}Se_2$ with shiny surfaces up to $1 \times 1 \times 0.2$ mm^3 can be grown. The crystals were characterized by x-ray diffraction (XRD) using a PANalytical diffractometer with Cu Kα radiation at room temperature. The average stoichiometry was determined by energy-dispersive x-ray (EDX) spectroscopy. DC magnetic susceptibility was measured from 10 K to 60 K using a Quantum Design PPMS-14. The resistivity from 2 K to 380 K was measured by a standard four-point probe technique using the Quantum Design PPMS-14, and above 380 K was measured with an alternative current resistance bridge (LR700P) by using a type-K chromel-alumel thermocouple as a thermometer in a vacuum oven. Microstructure investigations were performed on an FEI Tecnai-F20 transmission electron microscope (TEM) equipped with a double-tilt holder. The TEM samples were prepared in the glove box by gently crushing the single crystals.

III. RESULTS AND DISCUSSION

Figure 1 shows the XRD pattern for the single-crystal grown from the nominal composition $Na_{0.6}Fe_2Se_2$ (batch 1). Only the (00*l*) reflections can be recognized, which indicates that the crystals were perfectly oriented along the *c* axis. The lattice

*gfchen@aphy.iphy.ac.cn

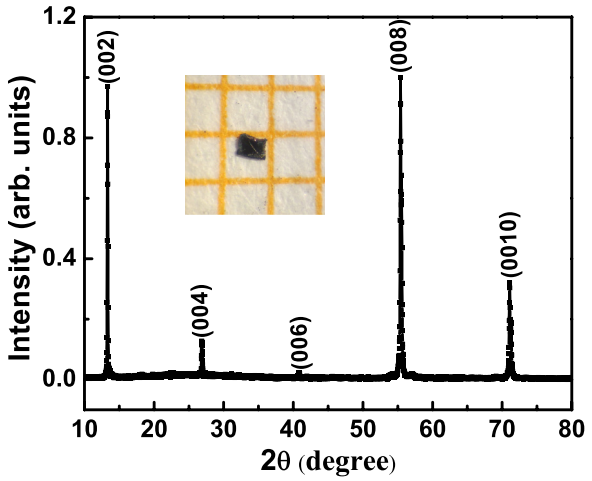

FIG. 1. (Color online) Single-crystal XRD pattern of $Na_{0.8}Fe_{1.6}Se_2$ (sample 1A) taken at room temperature. The inset shows a crystal with the typical dimension of 0.6 × 0.5 × 0.2 mm^3.

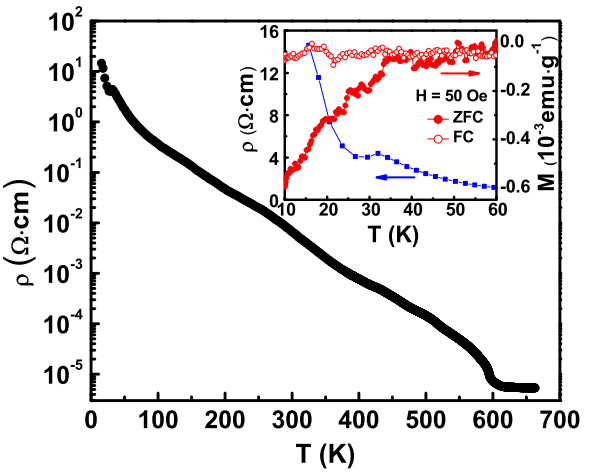

FIG. 3. (Color online) Temperature dependence of the in-plane resistivity (log scale) for $Na_{0.8}Fe_{1.6}Se_2$ (sample 2A). The inset shows the temperature dependance of in-plane resistivity and magnetization measured with a magnetic field of 50 Oe applied parallel to the c axis from 10 K to 60 K.

parameters of $a = 8.62$ Å, $c = 13.25$ Å were calculated based on space group $I4/m(87)$ from powder XRD data collected at room temperature (not shown here). It can be seen that the lattice parameters are evidently smaller than those observed in the K counterpart [20], which is reasonable because the Na ion has a much smaller radius than the K ion. The average atomic ratio determined from EDX is Na : Fe : Se = 0.82 : 1.636 : 2 (close to 2 : 4 : 5), which is consistent with that of the other 245 iron selenides and indicates that this compound is a 245 family member. Thus we write in the more familiar notation $Na_{0.8}Fe_{1.6}Se_2$ for this sample.

Figure 2 gives the in-plane resistivity as the function of temperature for single-crystal $Na_{0.8}Fe_{1.6}Se_2$ which is picked up from batch 1 (sample 1B). It increases rapidly with decreasing temperature and exhibits semiconducting characteristics. This in-plane resistivity can be described by an Arrhenius temperature dependence, $\rho = \rho_0 \exp(E_a/k_BT)$, where k_B is the Boltzmann constant. The activation energy E_a was estimated to be 183.6 meV (the fitting line shown as the inset of Fig. 2), which is larger than the activation energy of $TlFe_{1.3}Se_2 \sim$ 80.2 meV [6].

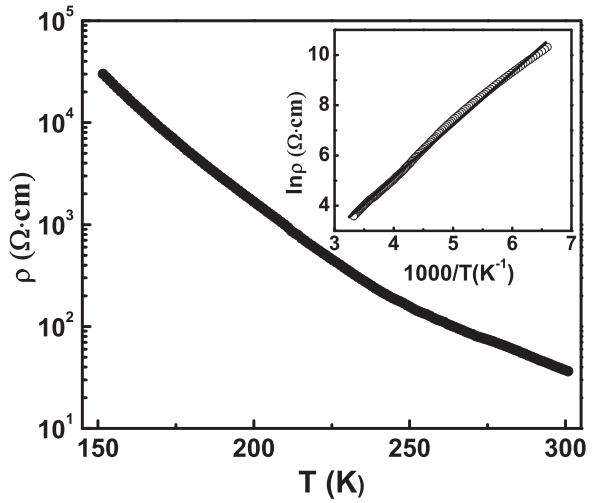

FIG. 2. Temperature dependence of the in-plane resistivity (log scale) for single crystal $Na_{0.8}Fe_{1.6}Se_2$ (sample 1B). Inset: lnρ as a function of $1/T$.

In $K_{1-x}Fe_{2-y}Se_2$, due to the presence of phase separation, by varying the contents of K and Fe, the volume fraction of different phases changes and the resistivity exhibits different characteristics (from metallic-superconducting to semiconducting/insulating) [21]. A similar approach was used to investigate the possible superconductivity in $Na_{1-x}Fe_{2-y}Se_2$. However, our systematic results show that the contents of Na and Fe in the prepared single crystal cannot be efficiently controlled by tuning the nominal composition in the starting materials, due to the formation of the $Na_3Fe_2Se_4$ in the batch. Fortunately, a small volume fraction of the superconducting phase can be detected for the sample grown from the nominal composition of $Na_{0.6}Fe_{2.1}Se_2$ (batch 2), as shown in Fig. 3. Although we cannot rule out other possibilities due to the small fractions of the superconducting component in the sample, we believe that superconductivity can be deduced in the $Na_xFe_2Se_2$ system via proper chemical tuning, similarly as in the well-studied $Am_xFe_2Se_2$ [4–6]. The superconducting transition temperature T_c inferred from the weak diamagnetic signal and the resistivity anomaly is ∼34 K (the inset of Fig. 3), which is slightly higher than potassium iron-selenide compounds. Due to the much smaller ionic radius of Na (0.95 Å), in comparison with K (1.33 Å), although the superconducting phase can still be found to coexist with the 245 phase in a similar phase-separated manner, the content is dramatically decreased. It has been previously reported that the Na and NH_3 molecules can be co-intercalated between the FeSe layers to form a $ThCr_2Si_2$-type superconducting phase with T_c at about 46 K [22]. Our result further indicates that the decrease of ionic radius disfavors the formation of the stable $ThCr_2Si_2$-type $Am_xFe_2Se_2$ phase.

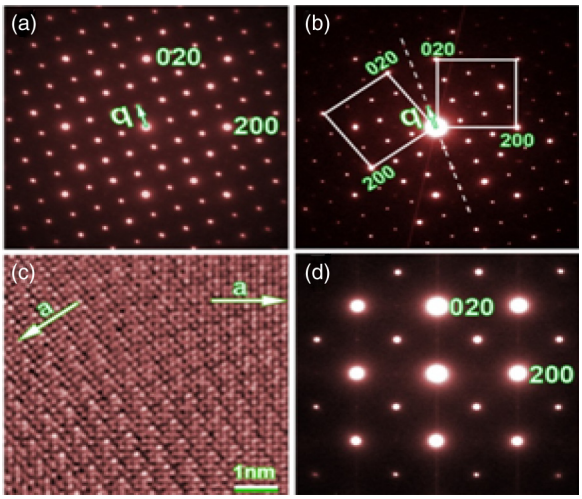

FIG. 4. (Color online) (a) Electron diffraction patterns of $Na_{0.8}Fe_{1.6}Se_2$ (sample 2B) taken along the [001] zone-axis direction, displaying the typical modulation of $q = 1/5(3a^* + b^*)$ due to the Fe-vacancy ordering in the Fe-Se layer. (b) Electron diffraction pattern and (c) high-resolution TEM images taken from a twinned area. (d) Electron diffraction pattern taken from small fraction of samples, showing the basic unit cell with no superstructure within the a^*-b^* reciprocal plane.

The temperature dependence of the in-plane resistivity for sample 2A at temperatures up to 650 K is plotted in Fig. 3. A structural transition takes place at $T_s = 595$ K, below which the resistivity begins to increase sharply. The structural transition in other 245 materials $Am_{0.8}Fe_{2-y}Se_2$ (Am = Cs, Rb, and K) have been determined by resistivity measurement with $T_s =$ 525 K, 540 K, and 551 K, respectively [7], which becomes higher with the decreasing of the lattice parameters. Therefore, the much higher T_s of $Na_{0.8}Fe_{1.6}Se_2$ is reasonable considering the appreciably smaller lattice parameters.

In order to better understand the correlation between the microstructural features and the physical properties in the present system, we performed TEM observations at room temperature. Figure 4(a) shows typical SAED patterns taken from a number of crystals picked up from batch 2 along the [001] zone axis direction, illustrating the structural features of this sample. The main diffraction spots with relatively strong intensity can be well indexed by the known tetragonal structure, which is consistent with the x-ray-diffraction results. It is recognizable that, in addition to the main diffraction spots, superlattice spots with wave vector $q = (3/5,1/5,0)$ are clearly visible in the a^*-b^* plane of reciprocal space, which are very similar to the superlattice spots reported for $K_{1-x}Fe_{2-y}Se_2$ [8] caused by Fe-vacancy ordering in the Fe-Se layer. Another notable structural feature observed in our TEM investigations is the structural twinning, which could give rise to interesting microstructure phenomena as illustrated in Figs. 4(b) and 4(c). Electron diffraction observations occasionally reveal a well-defined basic unit cell with no superstructure as shown in Fig. 4(d), which is possibly connected with a small fraction of superconducting phase observed in the $\chi(T)$ and $\rho(T)$ measurements.

IV. CONCLUSIONS

In conclusion, a layered iron-selenide $Na_{0.8}Fe_{1.6}Se_2$ single crystal has been successfully synthesized. TEM and XRD measurements show that, similarly to $K_{0.8}Fe_{1.6}Se_2$, $Na_{0.8}Fe_{1.6}Se_2$ also demonstrates evident superstructure along the [310] direction caused by Fe vacancy ordering; the anomaly observed at about 595 K in the resistivity measurement is likely caused by the Fe vacancy disorder-order transition. Moreover, a small volume of superconducting phase with $T_c \sim 34$ K could be produced by varying the contents of Na and Fe of the starting materials.

ACKNOWLEDGMENTS

This work is supported by the Strategic Priority Research Program of the Chinese Academy of Sciences (XDB07020000), the Fundamental Research Funds for the Central Universities, and the Research Funds of Renmin University of China (14XNH064).

[1] F. C. Hsu, J. Y. Luo, K. W. Yeh, T. K. Chen, T. W. Huang, P. M. Wu, Y. C. Lee, Y. L. Huang, Y. Y. Chu, D. C. Yan, and M. K. Wu, Proc. Natl. Acad. Sci. USA **105**, 14262 (2008).

[2] S. Medvedev, T. M. McQueen, I. A. Troyan, T. Palasyuk, M. I. Eremets, R. J. Cava, S. Naghavi, F. Casper, V. Ksenofontov, G. Wortmann, and C. Felse, Nat. Mater. **8**, 630 (2009).

[3] Q. Y. Wang, Z. Li, W. H. Zhang, Z. C. Zhang, J. S. Zhang, W. Li, H. Ding, Y. B. Ou, P. Deng, K. Chang, J. Wen, C. L. Song, K. He, J. F. Jia, S. H. Jia, Y. Y. Wang, L. L. Wang, X. Chen, X. C. Ma, and Q. K. Xue, Chin. Phys. Lett. **29**, 037402 (2012).

[4] J. Guo, S. Jin, G. Wang, S. Wang, K. Zhu, T. Zhou, M. He, and X. Chen, Phys. Rev. B **82**, 180520 (2010).

[5] A. Krzton-Maziopa, Z. Shermadini, E. Pomjakushina, V. Pomjakushin, M. Bendele, A. Amato, R. Khasanov, H. Luetkens, and K. Conder, J. Phys.: Condens. Matter **23**, 052203 (2011).

[6] M.-H. Fang, H.-D. Wang, C.-H. Dong, Z.-J. Li, C.-M. Feng, J. Chen, and H. Q. Yuan, Europhys. Lett. **94**, 27009 (2011).

[7] R. H. Liu, X. G. Luo, M. Zhang, A. F. Wang, J. J. Ying, X. F. Wang, Y. J. Yan, Z. J. Xiang, P. Cheng, G. J. Ye, Z. Y. Li, and X. H. Chen, Europhys. Lett. **94**, 27008 (2011).

[8] Z. Wang, Y. J. Song, H. L. Shi, Z. W. Wang, Z. Chen, H. F. Tian, G. F. Chen, J. G. Guo, H. X. Yang, and J. Q. Li, Phys. Rev. B **83**, 140505 (2011).

[9] P. Zavalij, Wei Bao, X. F. Wang, J. J. Ying, X. H. Chen, D. M. Wang, J. B. He, X. Q. Wang, G. F. Chen, P.-Y. Hsieh, Q. Huang, and M. A. Green, Phys. Rev. B **83**, 132509 (2011).

[10] W. Bao, Q. Z. Huang, G. F. Chen, M. A. Green, D. M. Wang, J. B. He, X. Q. Wang, and Y. M. Qiu, Chin. Phys. Lett. **28**, 086104 (2011).

[11] Y. Zhang, L. X. Yang, M. Xu, Z. R. Ye, F. Chen, C. He, H. C. Xu, J. Jiang, B. P. Xie, J. J. Ying, X. F. Wang, X. H. Chen, J. P.

Hu, M. Matsunami, S. Kimura, and D. L. Feng, Nat. Mater. **10**, 273 (2011).
[12] T. Qian, X.-P. Wang, W.-C. Jin, P. Zhang, P. Richard, G. Xu, X. Dai, Z. Fang, J.-G. Guo, X.-L. Chen, and H. Ding, Phys. Rev. Lett. **106**, 187001 (2011).
[13] K. Kuroki, S. Onari, R. Arita, H. Usui, Y. Tanaka, H. Kontani, and H. Aoki, Phys. Rev. Lett. **101**, 087004 (2008).
[14] I. I. Mazin, D. J. Singh, M. D. Johannes, and M. H. Du, Phys. Rev. Lett. **101**, 057003 (2008).
[15] W. Li, H. Ding, P. Deng, K. Chang, C. Song, K. He, L. Wang, X. Ma, J.-P. Hu, X. Chen, and Q.-K. Xue, Nat. Phys. **8**, 126 (2012).
[16] Y. Texier, J. Deisenhofer, V. Tsurkan, A. Loidl, D. S. Inosov, G. Friemel, and J. Bobroff, Phys. Rev. Lett. **108**, 237002 (2012).
[17] R. H. Yuan, T. Dong, Y. J. Song, P. Zheng, G. F. Chen, J. P. Hu, J. Q. Li, and N. L. Wang, Sci. Rep. **2**, 221 (2012).
[18] Z. Wang, Y. Cai, H. X. Yang, H. F. Tian, Z. W. Wang, C. Ma, Z. Chen, and J. Q. Li, Chin. Phys. B **22**, 087409 (2013).
[19] J. Zhao, H. Cao, E. Bourret-Courchesne, D.-H. Lee, and R. J. Birgeneau, Phys. Rev. Lett. **109**, 267003 (2012).
[20] Y. J. Song, Z. Wang, Z. W. Wang, H. L. Shi, Z. Chen, H. F. Tian, G. F. Chen, H. X. Yang, and J. Q. Li, Europhys. Lett. **95**, 37007 (2011).
[21] D. M. Wang, J. B. He, T.-L. Xia, and G. F. Chen, Phys. Rev. B **83**, 132502 (2011).
[22] T. P. Ying, X. L. Chen, G. Wang, S. F. Jin, T. T. Zhou, X. F. Lai, H. Zhang, and W. Y. Wang, Sci. Rep. **2**, 426 (2012).